Chaos
An Interdisciplinary Journal of Nonlinear Science

RESEARCH ARTICLE | JANUARY 21 2026

Reverse Newhouse–Ruelle–Takens route to chaos and time-dependent Hamiltonian formulation of a generalized Muthuswamy–Chua system

Bharathwaj Muthuswamy ; Jean-Marc Ginoux ; Roberto Concas ; Riccardo Meucci ; Jaume Llibre ; Leon O. Chua

Chaos 36, 013132 (2026)
https://doi.org/10.1063/5.0304010

Reverse Newhouse–Ruelle–Takens route to chaos and time-dependent Hamiltonian formulation of a generalized Muthuswamy–Chua system

Cite as: Chaos 36, 013132 (2026); doi: 10.1063/5.0304010
Submitted: 25 September 2025 · Accepted: 4 January 2026 ·
Published Online: 21 January 2026

Bharathwaj Muthuswamy,[1,a] Jean-Marc Ginoux,[2,b] Roberto Concas,[3,c] Riccardo Meucci,[4] Jaume Llibre,[5] and Leon O. Chua[6]

AFFILIATIONS

[1]NERD, Inc. (Nonlinear Engineering Research and Development), San Jose, California 95121, USA
[2]Université de Toulon, Aix Marseille Univ., CNRS, LIS, Toulon, France
[3]Istituto Nazionale di Ricerca Metrologica, Sesto Fiorentino, Florence, Italy
[4]National Institute of Optics—CNR, Florence, Italy
[5]Departament de Matemàtiques, Universitat Autònoma de Barcelona, 08193 Bellaterra, Barcelona, Spain
[6]Department of EECS, University of California, Berkeley, Berkeley, California 94720, USA

[a]**Electronic mail:** bharath@nerd-inc.org
[b]**Author to whom correspondence should be addressed:** jmginoux@orange.fr
[c]**Electronic mail:** r.concas@inrim.it

ABSTRACT

This work introduces a generalization of the Muthuswamy–Chua system of equations. The generalization allows us to embed memristive/hysteretic systems in a time-varying Hamiltonian, which acts as an energy-like Lyapunov function, whose growth or decay is governed by the memristor feedback and by whether the oscillator is momentarily kinetic- or potential-dominated. We perform mathematical analysis and detailed numerical investigations of the fourth-order Muthuswamy–Chua system based on bifurcation diagram and Lyapunov characteristic exponents. We then highlight bifurcation routes from torus breakdown to homoclinic chaos following the Newhouse–Ruelle–Takens scenario. The corresponding electronic oscillator is then analyzed and validated by SPICE (Simulation Program with Integrated Circuit Emphasis) simulations. To our knowledge, our work represents a novel memristive approach to describing a harmonic oscillator interacting with a finite "bath."

In this work, we present a generalization of the Muthuswamy–Chua memristive oscillator by coupling an external mass–spring pair to one harmonic oscillator "bath." By varying the control parameter, we highlight that the resulting four-dimensional model exhibits a reverse Newhouse–Ruelle–Takens (NRT) route to chaos. Then, while using the Helmholtz theorem, we deduce the energy function of this model, which is consistent with the Hamiltonian function obtained with the Caldirola–Kanai method. This leads us to the conclusion that a single-equilibrium memristive oscillator can self-pump energy through its internal bath, driving the reversed NRT cascade and furnishing a Lyapunov-like Hamiltonian that can be a springboard for quantization.

I. INTRODUCTION

The study of transition routes to chaos has been a central theme in nonlinear science for more than five decades. Following the seminal scenario proposed by Newhouse, Ruelle, and Takens,[1] several mechanisms leading from regular to chaotic dynamics have been identified in both physical and electronic systems. In particular, the breakdown of invariant tori, as clarified by Afraimovich and Shilnikov,[2] has played a fundamental role in understanding how quasiperiodic motion evolves into complex attractors. Parallel to these developments, the discovery of memristors and their incorporation into circuit theory[3] have provided simple yet powerful prototypes for exploring nonlinear and chaotic behavior. Among

these, the Muthuswamy–Chua (MC) system[3]—derived from the minimal inductor–capacitor–memristor topology—has emerged as a paradigmatic model capable of reproducing chaos with a low-dimensional structure. Its generalizations have been studied from the perspectives of integrability,[4] energy functions,[5–7] and Hamiltonian formulation,[8,9] thereby highlighting the deep connection between memory, dissipation, and conservative dynamics. Despite its apparent simplicity, the MC system continues to reveal new behaviors when extended to higher dimensions or when recast within generalized Hamiltonian frameworks. These extensions are not only relevant to circuit theory but also to a broader class of physical systems where memory effects mediate energy exchange between subsystems. In this paper, we propose a generalized four-dimensional MC oscillator in which an external harmonic oscillator is coupled to a finite "bath" representing the internal states of the memristor. Through bifurcation analysis, Lyapunov exponents, and numerical simulations, we demonstrate that this model undergoes a reverse Newhouse–Ruelle–Takens route to chaos. Moreover, by applying Helmholtz's theorem and the Caldirola–Kanai approach, we derive both an energy function and a time-dependent Hamiltonian, and we validate our theoretical predictions via an electronic circuit implementation and SPICE (Simulation Program with Integrated Circuit Emphasis) simulations.

II. THE MODEL

The Muthuswamy–Chua (MC) system of equations[4] are derived from the simplest topologically possible chaotic circuit[3]—an inductor–capacitor–memristor in series (parallel). The system equations are given below. Note that we have used notation commonly used in mechanics. Although the original MC system is obtained from an electronic circuit, the system equations are general and independent of the physical implementation. We chose mechanics since the goal of this work is to study a time-dependent Hamiltonian associated with the generalized MC system. Variable x is the position, and p is the momentum. $\mathbf{z}$ still represents the internal state of the memristor, and m and ω_0 are parameters (commonly referred to as mass and angular frequency, respectively) associated with the harmonic oscillator,

$$\begin{aligned} \frac{dx}{dt} &= \frac{p}{m}, \\ \frac{dp}{dt} &= -m\omega_0^2 x + \mu R(\mathbf{z})\, p, \\ \dot{\mathbf{z}} &= h(\mathbf{z}, p), \end{aligned} \tag{1}$$

where $\mu \in \mathbb{R}$. We will now define the following structure for R and h, $k \in \mathbb{N}$:

$$\begin{aligned} R(\mathbf{z}) &= \sum_{n=1}^{2k} a_n z_n, \\ \dot{z}_n &= z_{n+1}, \\ \dot{z}_{n+1} &= -z_n, \end{aligned} \tag{2}$$

where $a_n \in \mathbb{R}$. In the remainder of this work, we will use only $k = 1$, and so we have

$$\begin{aligned} R(z_1, z_2) &= a_1 z_1 + a_2 z_2, \\ \dot{z}_1 &= z_2, \\ \dot{z}_2 &= -z_1. \end{aligned} \tag{3}$$

Then, we obtain the following generalized Muthuswamy–Chua dynamical system:

$$\begin{aligned} \frac{dx}{dt} &= \frac{y}{m}, \\ \frac{dy}{dt} &= -m\omega_0^2 x + \mu\,(a_1 z + a_2 u)\, y, \\ \frac{dz}{dt} &= u, \\ \frac{du}{dt} &= -z, \end{aligned} \tag{4}$$

where we have posed: $p = y$, $z_1 = z$, and $z_2 = u$ for the sake of simplicity. Let us notice that this system (4) can also be written as

$$\begin{aligned} \frac{dx}{dt} &= \frac{y}{m}, \\ \frac{dy}{dt} &= -m\omega_0^2 x + \mu\,(a_1 \sin(t) + a_2 \cos(t))\, y, \end{aligned} \tag{5}$$

where $z(t) = \sin(t)$ and $u(t) = \cos(t)$. Thus, system (4) is, in fact, an external simple harmonic oscillator coupled to a memristive system whose internal states themselves are modeled by a finite "bath" of simple harmonic oscillator. We have chosen the simplest possible memristance function R, as a linear combination of the internal memristor states, for coupling the external harmonic oscillator with the memristor. When $\mu = 0$, the simple harmonic oscillator and the memristive system are uncoupled. That the solution of the simple harmonic oscillator is $x(t) = \cos(\omega_0 t)$, we have chosen the initial conditions $x(0) = 1$ and $y(0) = 0$. Concerning the memristive system, in order to obtain $z(t) = \sin(t)$ and $u(t) = \cos(t)$, initial conditions must be $z(0) = 0$ and $u(0) = 1$. Then, to observe chaotic dynamics with SPICE simulation, we will use these same initial conditions in Sec. V.

In some recent publications, we proposed a method for obtaining the *energy function* of any differential systems starting from their corresponding *equation of motion*, i.e., their *acceleration equation* in dimension two and *jerk equation* in dimension three.[5–7,10] In this work, we will extend these previous results to the system (4) of dimension four. To this aim, we will first consider the following set of nonlinear ordinary differential equations:

$$\frac{d\vec{X}}{dt} = \overrightarrow{\Im}(\vec{X}), \tag{6}$$

with $\vec{X} = [x_1, x_2, \ldots, x_n]^t \in E \subset \mathbb{R}^n$ and $\overrightarrow{\Im}(\vec{X}) = \left[f_1(\vec{X}), f_2(\vec{X}), \ldots, f_n(\vec{X})\right]^t \in E \subset \mathbb{R}^n$. The vector $\overrightarrow{\Im}(\vec{X})$ defines a velocity vector field $\dot{\vec{X}} = [\dot{x}_1, \dot{x}_2, \ldots, \dot{x}_n]^t$ in E whose components f_i, which are supposed to be infinitely differentiable with respect to all x_i, i.e., are C^∞ functions in E and with values included in $\mathbb{R}$. Components f_i satisfy the

assumptions of the Cauchy–Lipschitz theorem. For more details, see, for example, Coddington and Levinson.[11] In dimension two, it is well-known that the *energy function* of differential systems can be simply obtained by multiplying its corresponding second-order ordinary differential equation, i.e., its *equation of motion* by the first time derivative of its *state variable*. In dimension three, we have proved in our previous work[6] that the *jerk equation* of such differential systems must be multiplied by the second time derivative of the *state variable* and not by the first like in dimension two to obtain the *energy function*. However, nearly 40 years ago, Kobe[12] proposed to use a method based on Helmholtz's theorem to deduce the *energy function* of any n-dimensional differential systems (6). This method is briefly recalled below and was then re-used by Sarasola *et al.*,[13] Wang *et al.*,[8] Ma *et al.*,[9] and Yu *et al.*,[14] to name but a few. According to Helmholtz's theorem, such a differential system (6) can be decomposed into a gradient and a rotational field, i.e., as the sum of a conservative and dissipative vector field $\vec{\Im}(\vec{X}) = \vec{\Im}_c(\vec{X}) + \vec{\Im}_d(\vec{X})$. Thus, it can be expressed in a generalized Hamiltonian form,

$$\frac{d\vec{X}}{dt} = \left[J(\vec{X}) + R(\vec{X})\right]\nabla H(\vec{X}), \tag{7}$$

where ∇H is the gradient vector of the smooth *energy function* $H(\vec{X})$, $J(\vec{X})$ is a skew-symmetric matrix, and $R(\vec{X})$ is a symmetric matrix. The Hamiltonian *energy function* can, thus, be calculated by

$$\begin{aligned} \frac{dH}{dt} &= \nabla H^T R(\vec{X})\nabla H, \\ \nabla H^T J(\vec{X})\nabla H &= 0. \end{aligned} \tag{8}$$

Since the vector field (6) can be decomposed into a gradient and rotational field, it follows that the *energy function* and its rate of change can be deduced by

$$\begin{aligned} \frac{dH}{dt} &= \nabla H^T R(\vec{X})\nabla H = \nabla H^T \vec{\Im}_d(\vec{X}), \\ \nabla H^T J(\vec{X})\nabla H &= 0 = \nabla H^T \vec{\Im}_c(\vec{X}). \end{aligned} \tag{9}$$

III. STABILITY ANALYSIS

A. Fixed points

The unique fixed point is the origin $O(0, 0, 0, 0)$.

B. Jacobian matrix

The Jacobian matrix of dynamical system (4) reads

$$J = \begin{pmatrix} 0 & \frac{1}{m} & 0 & 0 \\ -m\omega_0^2 & \mu(a_1 z + a_2 y) & \mu a_1 y & \mu a_2 y \\ 0 & 0 & 0 & 1 \\ 0 & 0 & -1 & 0 \end{pmatrix}. \tag{10}$$

By replacing the coordinate of the fixed point O in the Jacobian matrix (4), one obtains the following four eigenvalues:

$$\lambda_{1,2} = \pm i; \quad \lambda_{3,4} = \pm i\omega_0.$$

Thus, the origin is *focus*. Moreover, it appears that no Hopf bifurcation can occur in our model (4). It follows that μ can be chosen as a *control parameter*.

1. Bifurcation diagram

In order to highlight the effects of the control parameter μ changes on the topology of the attractor of our model (4), we built a bifurcation diagram for the parameter set $m = 1$, $\omega_0 = 1$, $a_1 = 1.5$ and $a_2 = 0.25$. In Fig. 1, $x_{\max}(t)$ is plotted as a function of μ.

From $\mu = 0.01$ to $\mu = 1$, we observe a transition from a periodic orbit (limit cycle) to a chaotic attractor. To highlight this result, the phase portrait of the attractor of model (4) has been plotted in Fig. 3. For $\mu = 0.01$, the attractor is a *limit cycle*. Then, for $\mu = 0.4$, it becomes a torus. By reaching the value of $\mu = 0.75$, we observe a *homoclinic orbit*, and so, each equilibrium point is associated with the mentioned *homoclinic orbit*. Then, for $\mu = 1$, we observe a *chaotic attractor*.

In order to highlight the *sensitivity to initial conditions*, we have plotted in Fig. 2 the time series of model (4) for $\mu = 1$, $m = 1$,

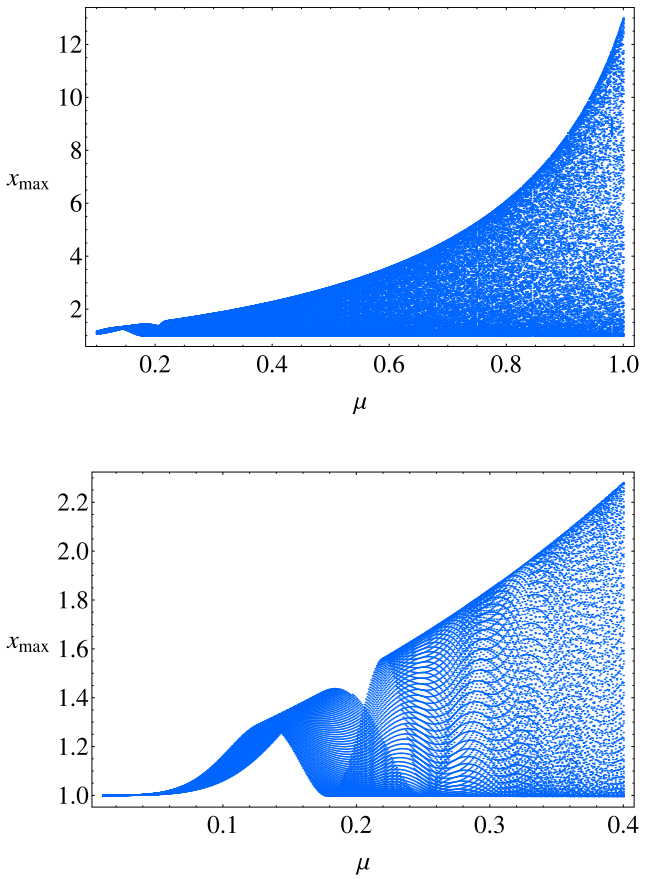

FIG. 1. Bifurcation diagram of model (4) for $m = 1$, $\omega_0 = 1$, $a_1 = 1.5$, and $a_2 = 0.25$.

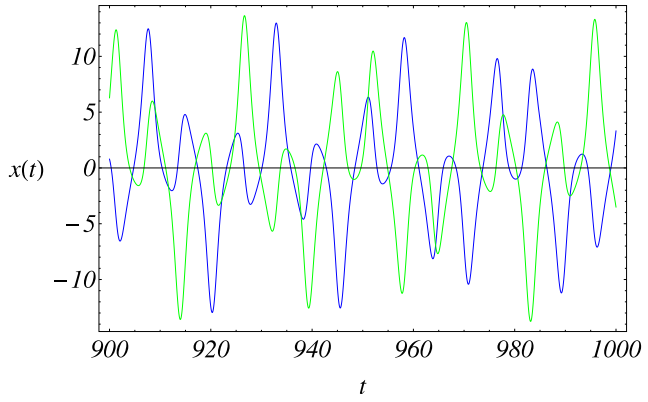

FIG. 2. Time series $x(t)$ of model (4) for $\mu = 1$, $m = 1$, $\omega_0 = 1$, $a_1 = 1.5$ and $a_2 = 0.25$.

$\omega_0 = 1$, $a_1 = 1.5$, and $a_2 = 0.25$, with $x(0) = 1$, $y(0) = 0$, $z(0) = 0$, $u(0) = 1$ in blue and with the same initial conditions except $u(0) = 1.01$ in green.

By reading from left to right the bifurcation diagram presented in Fig. 1 and comparing it to the phase portraits plotted in Fig. 3, topological changes of the trajectory curve, an integral of a dynamical system (4), seem to follow this route to chaos,

Limit Cycle (LC) $\Rightarrow$ Torus (T) $\Rightarrow$ Homoclinic Chaos (H).

In order to confirm such a scenario, Lyapunov Characteristic Exponents (LCEs) have been computed in each case.

2. Numerical computation of the Lyapunov exponents

The algorithm developed by Sandri[15] for Mathematica has been used to perform the numerical calculation of the Lyapunov characteristic exponents (LCEs) of model (4) in each case. Sandri's algorithm adopts the algorithm discussed in Ref. 16, which relies on the calculation of the order-p LCEs and the repeated application of the Gram–Schmidt orthonormalization procedure. LCEs values have been computed within each considered interval ($\mu \in [0.01, 1]$). As an example, for $\mu = 0.01$, Sandri's algorithm has provided the following LCEs $(0, -, -, -)$, while for $\mu = 0.4$, it provided the following LCEs $(0, 0, -, -)$. For $\mu = 0.75$, LCEs are $(+, 0, 0, -)$ and for $\mu = 1$, LCEs are $(+, 0, 0, -)$. Then, according to Klein and Baier[17] (see Table I), the numerical computation of the Lyapunov spectrum of model (4) confirms the existence of a periodic motion (*limit cycle*) for $\mu = 0.01$, of 3-torus for $\mu = 0.4$, and of a heteroclinic orbit and a chaotic attractor for $0.75 \leq \mu \leq 1$. LCE values have also been computed with the Lyapunov Exponents Toolbox (LET) developed by Steve Siu for MATLABő and involving the two algorithms proposed by Wolf *et al.*[18] and Eckmann and Ruelle[1] (see https://fr.mathworks.com/matlabcentral/fileexchange/233-let). Results obtained by both algorithms are consistent.

TABLE I. Spectral types of continuous autonomous attractors, from Klein and Baier.[17]

Dimension	LCE spectrum	Dynamics of the attractor	Hausdorff dimension
N = 4	Hypertorus on T^3	$(0, -, -, -)$	$D = 3$
	Chaos on T^3	$(+, 0, -, -)$	$3 < D < 4$
	Hyperchaos C^2	$(+, +, 0, -)$	$3 < D < 4$

IV. ROUTE TO CHAOS: THE NEWHOUSE–RUELLE–TAKENS SCENARIO

The main results presented in Sec. III confirm, on the one hand, stability analysis and, on the other hand, the computation of the Lyapunov characteristics exponents, that the trajectory curve integral of the generalized Muthuswamy–Chua system (4) follows this route to chaos,

Limit Cycle (LC) $\Rightarrow$ Torus (T) $\Rightarrow$ Homoclinic Chaos (H).

This scenario, in which the appearance of chaos is followed by the breakdown of a 3-torus, corresponds exactly to that proposed by Newhouse, Ruelle, and Takens (NRT).[19] In the very beginning of the 1970s, Fenichel[20] had already shown that the torus always loses its smoothness before the breakdown. However, it was only 20 years later that Afraimovich and Shilnikov[2] mathematically studied this phenomenon and stated their famous theorem "on the breakdown of the torus." Then, many authors investigated the phenomena of 3-torus or T^3-breakdown in third-order torus circuits[21,22] as well as homoclinic chaos in electronic circuits.[23,24] The theorem of Afraimovich and Shilnikov[2] predicted that the oscillatory regimes in (4) can evolve along three different routes:

A. torus breakdown due to the loss of smoothness,
B. torus breakdown due to the period-doubling of the periodic orbit, and
C. torus breakdown due to the appearance of a homoclinic trajectory.

According to what precedes, in our model (4), torus breakdown is due to the appearance of a homoclinic trajectory (route C) for the values μ of the control parameter as exemplified in Figs. 1 and 3.

A homoclinic bifurcation has been originally studied by Andronov and Leontovich[25,26] and then by Arnold *et al.*[22] and Kuznetsov.[27] According to Kuznetsov, "the disappearance of a homoclinic orbit leads to the creation or destruction of one (or more) limit cycle nearby."[27] This is exactly what is observed in our model (4) for the values $\mu \in [0.01, 1]$ of the control parameter (see Fig. 3).

V. EXPERIMENTAL SETUP

The system of differential equations (4) describing the Muthuswamy–Chua memresistive oscillator model considered can be solved via analog computation by using SPICE simulations. Such an approach provides reliable results as demonstrated in Concas *et al.*[28] in simulating laser dynamics with several nonlinearities and in Ginoux *et al.*[10] in a simulating memristor model.

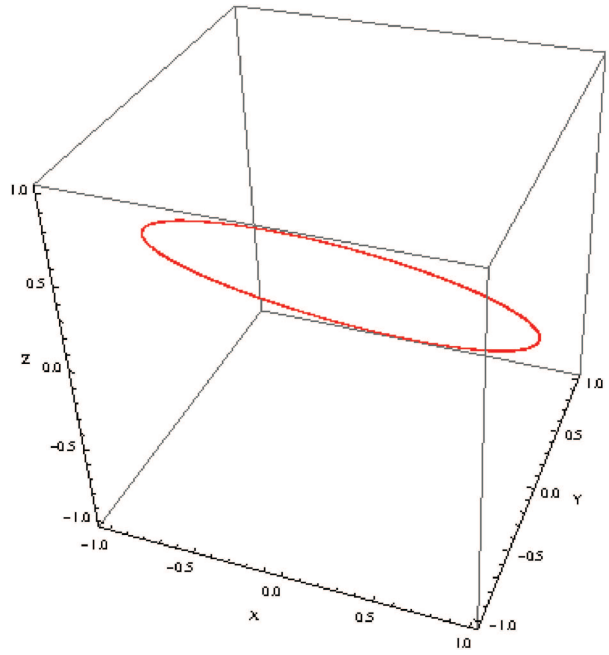

(a) $\mu = 0.01$

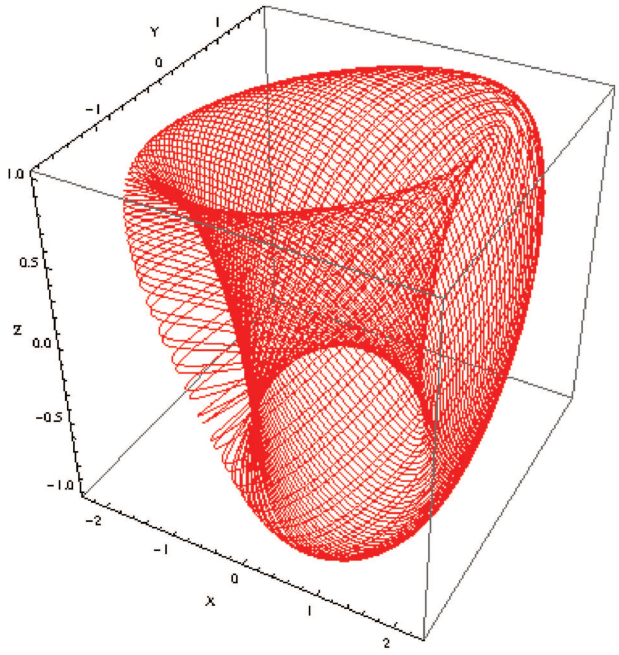

(b) $\mu = 0.4$

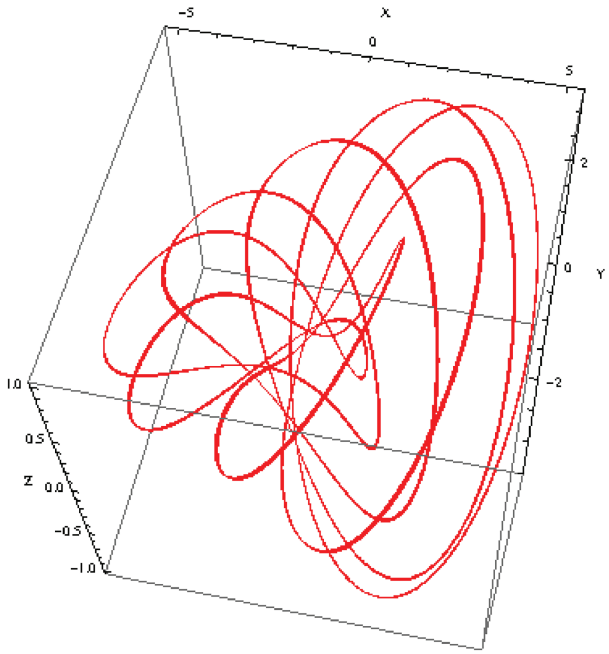

(c) $\mu = 0.75$

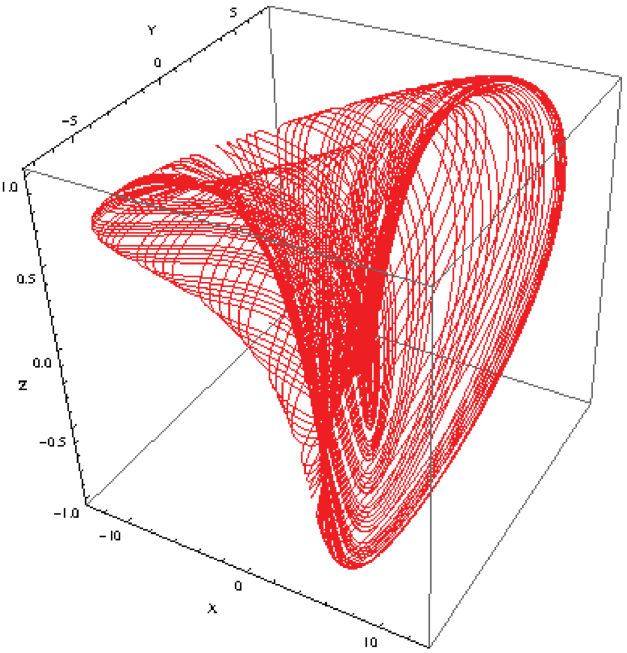

(d) $\mu = 1$

FIG. 3. Phase portraits of model (4) for various values μ. (a) $\mu = 0.01$. (b) $\mu = 0.4$. (c) $\mu = 0.75$. (d) $\mu = 1$.

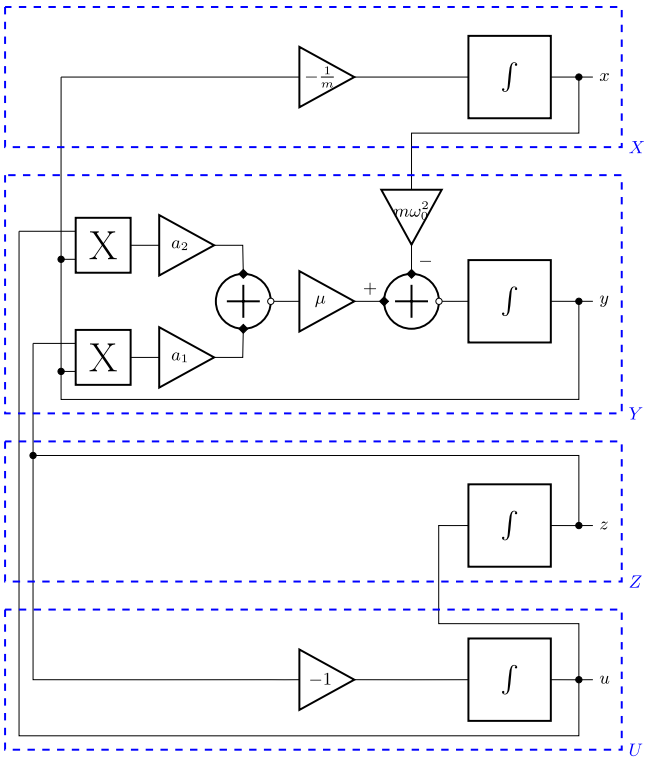

FIG. 4. Design block implementation of Eq. (4). The architecture consists of four functional blocks *X*, *Y*, *Z*, *U*, each enclosed by a blue, dashed box, where it implements the differential equations providing *x*, *y*, *z*, and *u*.

The block diagram shown in Fig. 4 provides a functional scheme of the system. It includes four ideal integration blocks whose outputs are the variables x, y, z, and u, two summing nodes, and the amplification blocks for $\frac{1}{m}$, $m\omega_0^2$, a_1, a_2, and μ. The nonlinear terms are realized by the multiplier blocks for ZY and UY.

A. Electronic circuit

The electronic circuit implementation of the circuit blocks introduced in Fig. 4 is shown in Fig. 5(a). All active components are assumed to be power supplied with ± 15 V. All operational amplifiers (op-amps) used in this circuit are the AD820.

The normally closed switches S_1, S_2, S_3, and S_4 are used to start the circuit with initial conditions for x, y, z, and u at $t = 0$, while the voltage sources E_1, E_2 define the initial condition values for x and u.

The nonlinear terms are obtained by using two identical blocks *M*1 and *M*2, and their scheme is shown in Fig. 5(b), each containing an analog multiplier AD633JN and a noninverting amplifier based on the op-amp *OA*.

The integrator producing x based on the op-amps IC1 is fed with the term y, and the op-amp IC2 provides its inversion. By using a standard analysis in the Laplace frequency domain where $s = j\omega$ and $\tilde{A}$ represent the Laplace transforms of a generic time-dependent

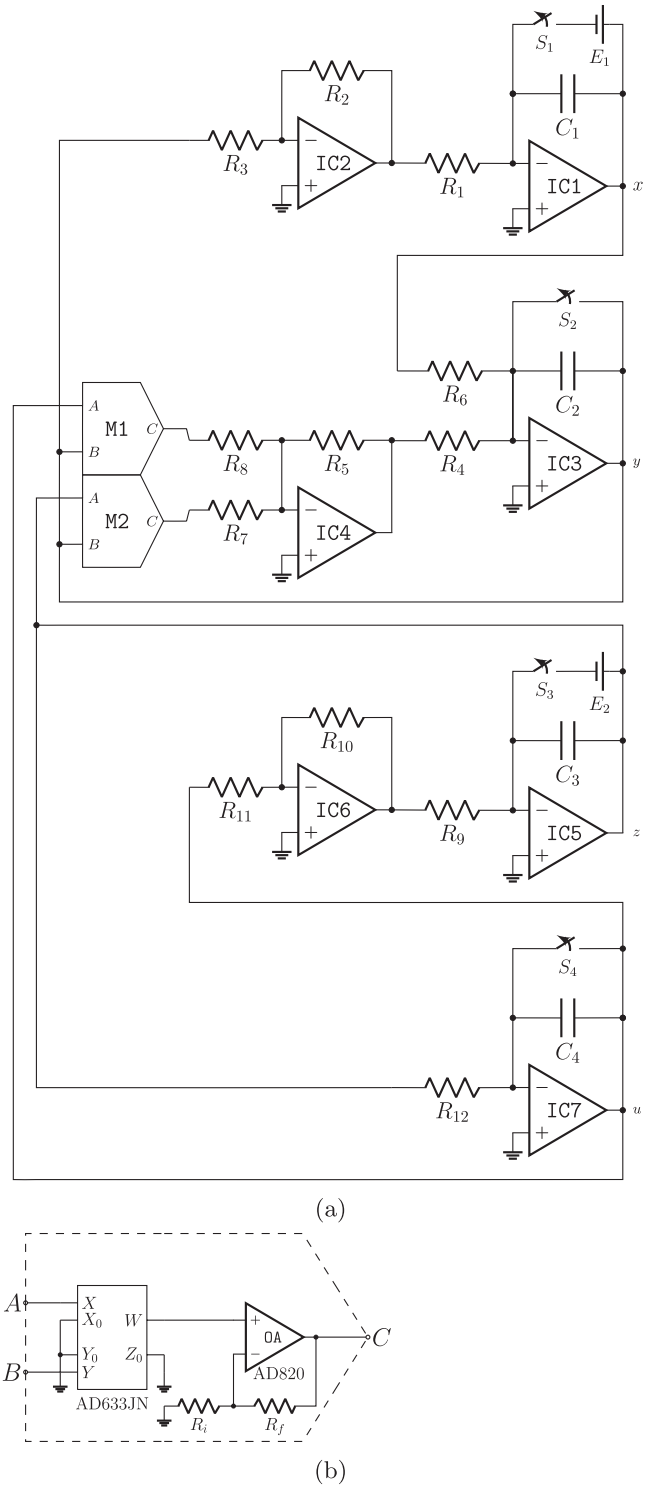

FIG. 5. Electronic circuit diagram and the multiplier embedded schematic.

function A, we obtain

$$s\tilde{x} = -\frac{1}{m}k'_x\tilde{y}. \tag{11}$$

The integrator producing y is based on the op-amp IC3 and is fed the term x and the sum of zy and uy by the use of the op-amp IC4. In the frequency domain, we have

$$s\tilde{y} = -m\omega_0^2\tilde{x} + \mu\left[a_1\widetilde{zy} + a_2\widetilde{uz}\right]. \tag{12}$$

The integrator producing z is based on the op-amp IC5 and is fed with the term u, and the op-amp IC6 provides its inversion. In the frequency domain, we have

$$s\tilde{z} = -k_z k'_z\tilde{u}. \tag{13}$$

The integrator producing u is based on the op-amp IC7 and is fed with the term z. In the frequency domain, we have

$$s\tilde{u} = -k_u\tilde{z}. \tag{14}$$

The dynamics of the circuit, expressed in the Laplace domain (s denotes a complex frequency), can be promptly derived as follows:

$$s\tilde{x} = -\frac{1}{R_1C_1}\left(-\frac{R_2}{R_3}\right)\tilde{y}, \tag{15a}$$

$$s\tilde{y} = -\frac{1}{R_6C_2}\tilde{x} - \frac{1}{R_4C_2}\left[-\frac{R_5}{R_7}\widetilde{zy} - \frac{R_5}{R_8}\widetilde{uy}\right], \tag{15b}$$

$$s\tilde{z} = -\frac{1}{R_9C_3}\left(-\frac{R_{10}}{R_{11}}\right)\tilde{u}, \tag{15c}$$

$$s\tilde{u} = -\frac{1}{R_{12}C_4}\tilde{z}, \tag{15d}$$

where $\tilde{x}$, $\tilde{y}$, $\tilde{z}$, and $\tilde{u}$ are the Laplace transforms of the voltages x, y, z, and u, respectively.

B. SPICE simulation

The analog electronic simulation was carried out by using the software SPICE-based LTSpice®, which allows to reliably simulate analog or digital electronic circuits by means of models of electronic components used therein. This type of electronic simulation can consider nonidealities and limits of the components, and it reproduces the full electronic behavior of op-amps and multipliers, such as output voltage dynamic, input offset voltage, slew rate, and multiplier's non-linearity. Consequently, simulations mostly faithfully reproduce what would result from real implementations.

TABLE II. Values of resistors and capacitors composing the passive network components of the circuit diagram, with the values used in simulation.

Component	Value	Component	Value	Component	Value
R_1	10 kΩ	R_7	6.67 kΩ	R_i	1.05 kΩ
R_2	10 kΩ	R_8	40 kΩ	R_f	9.53 kΩ
R_3	10 kΩ	R_9	10 kΩ	C_1	100 nF
R_4	Table III	R_{10}	10 kΩ	C_2	100 nF
R_5	10 kΩ	R_{11}	10 kΩ	C_3	100 nF
R_6	10 kΩ	R_{12}	10 kΩ	C_4	100 nF

TABLE III. Values of R_4 corresponding to μ values.

R_4	μ
1 MΩ	0.01
25 kΩ	0.4
13.3 kΩ	0.75
10 kΩ	1

Considering the design of Fig. 5, embedded SPICE models were used for both the passive components and the op-amps, whereas a basic SPICE model for multipliers was chosen.

In order to replicate the chaotic dynamics, the simulation has been started from the initial condition values defined in Eq. (16),

$$x(0) = 1\,\text{V}, \quad y(0) = 0\,\text{V}, \quad z(0) = 0\,\text{V}, \quad u(0) = 1\,\text{V}, \tag{16}$$

and consequently, the voltage values of the sources are

$$E_1 = 1\,\text{V}, \quad E_2 = 1\,\text{V}. \tag{17}$$

Once the boundary conditions are assigned, the simulation covers a span of 1 s. The component values are chosen to obtain the parameters

$$m = 1, \quad \omega_0 = 1, \tag{18a}$$

$$a_1 = 1.5, \quad a_2 = 0.25, \tag{18b}$$

$$\mu = [0.01, 0.4, 0.75, 1] \tag{18c}$$

and listed in Tables II and III.

The results of the electronic simulation results are displayed in Figs. 6(a)–6(d).

Figure 6 points at a remarkable similarity between the numerical integration and the SPICE simulation results confirming the robustness of the model.

VI. ENERGY FUNCTION OF THE GENERALIZED MUTHUSWAMY–CHUA SYSTEM

According to Helmholtz's theorem, the generalized Muthuswamy–Chua system (4) can be decomposed into a gradient and a rotational field, i.e., as the sum of conservative and dissipative vector fields as follows:

$$\begin{pmatrix}\dot{x}\\ \dot{y}\\ \dot{z}\\ \dot{u}\end{pmatrix} = \begin{pmatrix}0 & \frac{1}{m} & 0 & 0\\ -m\omega_0^2 & 0 & 0 & 0\\ 0 & 0 & 0 & 1\\ 0 & 0 & -1 & 0\end{pmatrix}\begin{pmatrix}x\\ y\\ z\\ u\end{pmatrix} + \begin{pmatrix}0\\ \mu\,(a_1z + a_2u)\,y\\ 0\\ 0\end{pmatrix}. \tag{19}$$

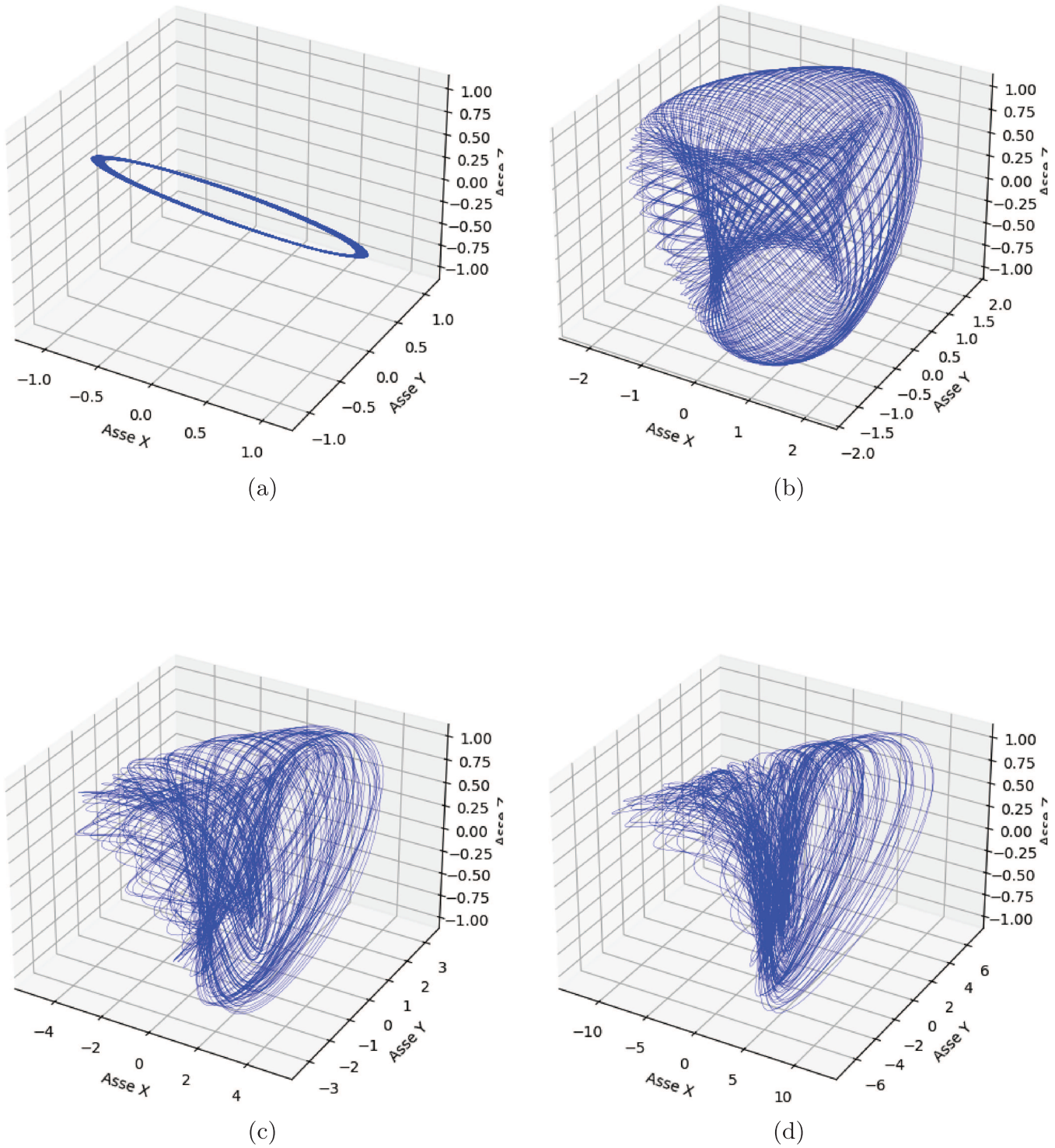

FIG. 6. SPICE simulation representing the attractor in phase space x–y–z of Eq. (4) at different values of μ: 0.01, 0.4, 0.75, and 1, respectively, in Figs. 6(a)–6(d).

Thus, the *energy function* H associated with the generalized Muthuswamy–Chua system (19) must satisfy the partial differential equation,

$$\left(\frac{\partial H}{\partial x},\frac{\partial H}{\partial y},\frac{\partial H}{\partial z},\frac{\partial H}{\partial u}\right)\begin{pmatrix}\frac{y}{m}\\ -m\omega_0^2 x\\ u\\ -z\end{pmatrix}=0\Leftrightarrow\begin{cases}\frac{\partial H}{\partial x}=m\omega_0^2 x,\\ \frac{\partial H}{\partial y}=\frac{y}{m},\\ \frac{\partial H}{\partial z}=z,\\ \frac{\partial H}{\partial u}=u.\end{cases}\tag{20}$$

This leads to the *energy function*

$$H=m\omega_0^2\frac{x^2}{2}+\frac{y^2}{2m}+\frac{z^2}{2}+\frac{u^2}{2}.\tag{21}$$

From (9), (8), and (7), the rate of change of the *energy function* is

$$\begin{aligned}\frac{dH}{dt}&=\left(\frac{\partial H}{\partial x},\frac{\partial H}{\partial y},\frac{\partial H}{\partial z},\frac{\partial H}{\partial u}\right)\begin{pmatrix}0\\ a_1zy+a_2uy\\ 0\\ 0\end{pmatrix}\\ &=\mu\left(a_1z+a_2u\right)\frac{y^2}{m}.\end{aligned}\tag{22}$$

However, as recalled above, the generalized Muthuswamy–Chua system (4) could also be written as

$$\begin{aligned}\frac{dx}{dt}&=\frac{y}{m},\\ \frac{dy}{dt}&=-m\omega_0^2x+\mu\left(a_1z+a_2u\right)y.\end{aligned}\tag{23}$$

By taking the time derivative of the first equation of (23), we obtain its corresponding *equation of motion* or *acceleration equation*,

$$\ddot{x}+\omega_0^2x=\mu\left(a_1z+a_2u\right)\dot{x}.\tag{24}$$

Multiplying Eq.(24) by $\dot{x}$ provides an alternative way to obtain the *energy function*. Thus, we have

$$\dot{x}\ddot{x}+\omega_0^2x\dot{x}=\mu\left(a_1z+a_2u\right)\dot{x}^2,\tag{25}$$

which can be written as

$$\frac{d}{dt}\left(\frac{\dot{x}^2}{2}+\omega_0^2\frac{x^2}{2}\right)=\mu\left(a_1z+a_2u\right).\dot{x}^2.\tag{26}$$

Thus, we obtain

$$H=\frac{\dot{x}^2}{2}+\omega_0^2\frac{x^2}{2}\quad\text{and}\quad\frac{dH}{dt}=\mu\left(a_1z+a_2u\right)\dot{x}^2.\tag{27}$$

At first sight, it could appear that both *energy function* and their rate of change (21) and (22), and (27) are different. In fact, while using the fact that, according to (4), $\dot{x}=y/m$, it is easy to verify that there is only a factor $1/m$ between them.

VII. TIME-VARYING HAMILTONIAN

To derive the time-varying Hamiltonian, we will use the Caldirola–Kanai (CK)[29,30] approach. Note that we will first use $z_1=z; z_2=u$ in the discussion below. Using a standard notation, for damped harmonic oscillators with constant γ, the CK Hamiltonian is given by

$$H(x,p,t)=e^{-\gamma}\frac{p^2}{2m}+\frac{1}{2}e^{\gamma}m\omega_0^2x^2.\tag{28}$$

Since the damping in the generalized MC system is confined to the memristor through R, let $\gamma(t)\equiv a_1z_2(t)-a_2z_1(t)$. We can show that the following H yields the system equations for the generalized MC system [assuming the definitions of R and $\mathbf{z}$ in Eq. (3)]:

$$H_{GMC}(x,p,t)=e^{-\gamma(t)}\frac{p^2}{2m}+\frac{1}{2}e^{\gamma(t)}\left(m\omega_0^2x^2\right).\tag{29}$$

To show that Eq. (29) does indeed give rise to system equations, we will first rewrite the generalized MC system [Eq. (1)] as a second-order differential equation in x, while using the definitions of R and $\mathbf{z}$ from Eq. (3),

$$\begin{aligned}\ddot{x}-(a_1z_1+a_2z_2)\dot{x}+\omega_0^2x&=0,\\ \dot{z}_1&=z_2,\\ \dot{z}_2&=-z_1.\end{aligned}\tag{30}$$

Now, from the definition of the Hamiltonian, we get

$$\begin{aligned}\dot{x}&=\frac{\partial H_{GMC}}{\partial p},\\ \dot{p}&=-\frac{\partial H_{GMC}}{\partial x}.\end{aligned}\tag{31}$$

Hence,

$$\dot{x}=e^{-\gamma(t)}\frac{p}{m},\tag{32}$$

$$\dot{p}=-m\omega_0^2xe^{\gamma(t)}.\tag{33}$$

Taking the second derivative of $\dot{x}$ above and simplifying, we get

$$\begin{aligned}\ddot{x}&=e^{-\gamma(t)}\frac{\dot{p}}{m}+\frac{p}{m}\left(\frac{d}{dt}e^{-\gamma(t)}\right)\\ &=e^{-\gamma(t)}\frac{\dot{p}}{m}-\frac{p}{m}e^{-\gamma(t)}\dot{\gamma}(t).\end{aligned}\tag{34}$$

Eliminating p and $\dot{p}$ using Eqs. (32) and (33), we get

$$\begin{aligned} \ddot{x} + \dot{\gamma}(t)\dot{x} + \omega_0^2 x = 0, \\ \ddot{x} + (a_1\dot{z}_2(t) - a_2\dot{z}_1(t))\dot{x} + \omega_0^2 x = 0. \end{aligned} \tag{35}$$

Now, since we *defined the internal memristor state equations as* $\dot{z}_1 \equiv z_2$, $\dot{z}_2 \equiv -z_1$, we see that Eq. (35) does indeed match the first equation in Eq. (30).

Note that we do not need to explicitly define conjugate momenta for $\dot{z}_1$, $\dot{z}_2$ from H_{GMC}, because H_{GMC} already generates the correct second-order equation for x. In other words, the memristive effect is built into the Hamiltonian via the time-dependent term $e^{-(a_1 z_2 - a_2 z_1)}$.

Now, let us compare the *time-varying Hamiltonian* H_{GMC} (29) and the *energy function* H (27). To this aim, let us pose $\mu = 1$ and $\tilde{\gamma} = a_1 z_1 + a_2 z_2$. Now, according to (29), we have

$$H_{GMC} = e^{-\gamma}\frac{p^2}{2m} + \frac{1}{2}e^{\gamma}\left(m\omega_0^2 x^2\right). \tag{36}$$

By using Eqs. (32) and (27), this equation reads

$$H_{GMC} = me^{\gamma}\left(\frac{\dot{x}^2}{2} + \omega_0^2\frac{x^2}{2}\right) = me^{\gamma}H. \tag{37}$$

Now, let us compute the rate of change of H_{GMC}. We have

$$\frac{dH_{GMC}}{dt} = m\left(\frac{d}{dt}e^{\gamma}\right)H + me^{\gamma}\frac{dH}{dt}. \tag{38}$$

Let us notice that using the definitions of γ, $\tilde{\gamma}$, and the internal state evolution of the memristor from (30),

$$\frac{d\gamma}{dt} = -\tilde{\gamma}. \tag{39}$$

According to (27), we have

$$\frac{dH}{dt} = \tilde{\gamma}\dot{x}^2. \tag{40}$$

It follows from Eqs. (39) and (40) that

$$\frac{dH_{GMC}}{dt} = -m\tilde{\gamma}e^{\gamma}H + m\tilde{\gamma}e^{\gamma}\dot{x}^2. \tag{41}$$

Factoring out $m\tilde{\gamma}e^{\gamma}$, we have

$$\frac{dH_{GMC}}{dt} = m\tilde{\gamma}e^{\gamma}\left(\dot{x}^2 - H\right). \tag{42}$$

Substituting for H from (27) and simplifying, we have

$$\frac{dH_{GMC}}{dt} = m\tilde{\gamma}e^{\gamma}\left(\frac{\dot{x}^2}{2} - \omega_0^2\frac{x^2}{2}\right). \tag{43}$$

Equation (43) shows that the time-varying Hamiltonian H_{GMC} acts as an *energy-like Lyapunov function, whose growth or decay is governed by the memristor feedback* $\tilde{\gamma}$ *and by whether the oscillator is momentarily kinetic- or potential-dominated. The sign changes of* $\tilde{\gamma}\left(\frac{\dot{x}^2}{2} - \omega_0^2\frac{x^2}{2}\right)$ *are precisely what allow bursts of energy injection that lead to the torus-breaking and homoclinic transitions documented earlier in the paper.*

Another interpretation of (43) follows from the definition of the *Lagrangian*[31] L,

$$L = \frac{1}{2}m\left(\dot{x}^2 - \omega_0^2 x^2\right) = T - V. \tag{44}$$

For *any* system with coordinates q_i and conjugate momenta p_i, the relationship between the Hamiltonian and the Lagrangian[31] is

$$\dot{H} = -\left.\frac{\partial L}{\partial t}\right|_{q_i,\dot{q}_i \text{ fixed}}, \tag{45}$$

which follows directly from the definition $H = \sum_i p_i\dot{q}_i - L$ and the Euler–Lagrange equations (see, e.g., Hamill,[31] Chap. 4).

To compute $\frac{\partial L}{\partial t}$, let us consider the following definition of an *effective Lagrangian*:

$$\tilde{L}(t) \equiv e^{\gamma(t)}L. \tag{46}$$

Computing the explicit time-dependence and using (39), along with the definition of the Lagrangian from (44), we get

$$-\left.\frac{\partial\tilde{L}}{\partial t}\right|_{x,\dot{x}} = -\dot{\gamma}e^{\gamma}L = -\tilde{\gamma}e^{\gamma}\frac{1}{2}m\left(\dot{x}^2 - \omega_0^2 x^2\right). \tag{47}$$

Here, the partial derivative $\frac{\partial\tilde{L}}{\partial t}$ is taken at fixed x and $\dot{x}$, as in Eq. (45). The bare Lagrangian $L = \frac{1}{2}m(\dot{x}^2 - \omega_0^2 x^2)$ has no explicit time dependence, so all explicit t-dependence comes from the prefactor $e^{\gamma(t)}$ in $\tilde{L}(t) = e^{\gamma(t)}L$. Therefore, we obtained Eq. (47) in which we used Eq. (39) for $\dot{\gamma}$.

From (43) and (47), we have

$$\dot{H}_{GMC} = -\frac{\partial\tilde{L}}{\partial t}. \tag{48}$$

Hence, the identity (45) is satisfied, confirming that the term $\tilde{\gamma}e^{\gamma}(T - V)$ is the "standard power input" arising from explicit time-dependence in the Lagrangian/Hamiltonian pair.

VIII. DISCUSSION

In this work, we generalized the Muthuswamy–Chua memristive oscillator to a four-dimensional form [Eq. (4)], that couples an external mass–spring pair (x, y) to one harmonic oscillator "bath" [represented by internal memristor states (z, u)], via a memristance function R that is a linear combination of internal memristor states. Then, numerical computations and Lyapunov analysis show a limit-cycle → 3-torus → homoclinic orbit → chaos progression when the coupling gain μ is increased. Decreasing u reproduces the canonical NRT route to chaos. The birth of a homoclinic orbit at $\mu \approx 0.75$ triggers torus breakdown and the onset of a robust chaotic attractor, consistent with route C of the Afraimovich–Shilnikov theorem. Then, using the Helmholtz theorem, we obtained an explicit scalar

energy H [Eq. (21)] and its balance law [Eq. (22)], generalizing earlier 2D/3D results to 4D. We obtained a Caldirola–Kanai like Hamiltonian H_{GMC} [Eq. (29)] that reproduces the full dynamics and its time derivative [Eq. (43)] matches the power input from the memristor feedback. We verified consistency with the Lagrangian, cementing the energy-balance interpretation and linking the Hamiltonian formalism to the bare oscillator Lagrangian $L = T - V$. Then, the SPICE simulations have enabled to reproduce the theoretical predictions of our model. Together, these results give a coherent classical picture: a single-equilibrium memristive oscillator can self-pump energy through its internal bath, driving the reversed NRT cascade and furnishing a Lyapunov-like Hamiltonian that can be a springboard for quantization.

The fact that $H_{GMC}(x, p, t)$ has the Caldirola–Kanai structure $H_{GMC} = e^{-\gamma(t)}p^2/2m + e^{\gamma(t)}m\omega_0^2x^2/2$ is also interesting from a quantum perspective. In the CK approach, such time-dependent Hamiltonians can be quantized in the usual way by promoting x and p to operators and solving the associated time-dependent Schrödinger equation for a damped oscillator. Our construction, therefore, provides a natural starting point ("springboard") for a future quantization program in which the generalized Muthuswamy–Chua oscillator is treated as a minimal model of a "quantum memristive oscillator" coupled to a finite bath. Exploring this quantum analog lies beyond the scope of the present classical study, but the existence of H_{GMC} shows that standard quantization schemes for time-dependent Hamiltonians can, in principle, be applied to this memristive system.

Other avenues for future work include providing firm proof of the global geometry underlying the reverse NRT route to chaos and quantitatively demarcating chaotic vs quasiperiodic regions. Then, we will search for hidden attractors and determine whether additional coexisting attractors exist whose basins do not intersect the equilibrium neighborhood. Another possibility could be to use higher-order baths and to extend the model to multiple (z_{2k-1}, z_{2k}) pairs. Concerning the nonlinear memristance $R(\mathbf{z})$, we could also replace linear combination with, say, polynomial R. In this paper, we analyzed the GMC system in a dimensionless form. For physical interpretations, a single rate scale μ (s^{-1}) must be carried explicitly. To see why this is so, let a_1, a_2, z_1, z_2 be dimensionless and recall our definitions of $R(z_1, z_2) = a_1z_1(t) + a_2z_2(t), \gamma(t) = a_1z_2(t) - a_2z_1(t)$. To ensure $[\gamma(t)] = 1$ (so that $e^{\pm\gamma}$ is well defined) and that the multiplier of p (i.e., μR) in $p' = -m\omega_0^2x + \mu Rp$ has units of s^{-1}, the coupling μ must carry units of s^{-1}. Hence, the internal states must evolve as

$$\begin{aligned} z_1' &= \mu z_2, \\ z_2' &= -\mu z_1, \end{aligned} \tag{49}$$

which yields $\gamma'(t) = -\mu R(z_1, z_2)$, and therefore, $p' = -m\omega_0^2x - \gamma' p$, consistent with the Caldirola–Kanai Hamiltonian $H = e^{-\gamma}\frac{p^2}{2m} + \frac{1}{2}m\omega_0^2x^2e^{\gamma}$. In the present work, we set $\mu = 1$ for simplicity. Thus, coefficients in R are dimensionless under this convention, so μR retains units of s^{-1}. A perspective to be given to this work is to analyze the possible new dynamical regimes of our model (4) when using different values of the parameters m, μ, ω_0, a_1, and a_2 as exemplified in the Appendix.

ACKNOWLEDGMENTS

The authors would like to thank the reviewers for their helpful advice, which enabled them to improve the quality of this work. J. Llibre is partially supported by the Agencia Estatal de Investigacion of Spain grant PID2022-136613NB-100.

AUTHOR DECLARATIONS

Conflict of Interest

The authors have no conflicts to disclose.

Author Contributions

Bharathwaj Muthuswamy: Conceptualization (equal); Formal analysis (equal); Investigation (equal); Methodology (equal); Validation (equal); Visualization (equal); Writing – original draft (equal); Writing – review & editing (equal). **Jean-Marc Ginoux:** Conceptualization (equal); Formal analysis (equal); Investigation (equal); Methodology (equal); Validation (equal); Visualization (equal); Writing – original draft (equal); Writing – review & editing (equal). **Roberto Concas:** Conceptualization (equal); Formal analysis (equal); Investigation (equal); Methodology (equal); Validation (equal); Visualization (equal); Writing – original draft (equal); Writing – review & editing (equal). **Riccardo Meucci:** Conceptualization (equal); Formal analysis (equal); Investigation (equal); Methodology (equal); Validation (equal); Visualization (equal); Writing – original draft (equal); Writing – review & editing (equal). **Jaume Llibre:** Conceptualization (equal); Formal analysis (equal); Investigation (equal); Methodology (equal); Validation (equal); Visualization (equal); Writing – original draft (equal); Writing – review & editing (equal). **Leon O. Chua:** Conceptualization (equal); Formal analysis (equal); Investigation (equal); Methodology (equal); Validation (equal); Visualization (equal); Writing – original draft (equal); Writing – review & editing (equal).

DATA AVAILABILITY

The data that support the findings of this study are available from the corresponding author upon reasonable request.

APPENDIX: BIFURCATION DIAGRAMS FOR OTHER PARAMETERS

In this Appendix, we discuss the possible new dynamical regimes (as those represented in the bifurcation diagram reported in Fig. 1) when using different values of the parameters m, ω_0, a_1, and a_2 (with respect to the chosen ones, i.e., when $\mu = 1$). Numerical investigations concerning the parameter m have shown that it acts as a *scale factor* for the variable y since it modifies its amplitude but does not seem to have any effect on the attractor shape. On the contrary, parameters a_1, a_2, and ω_0 have a great influence on the attractor shape. We have built the bifurcation diagrams for these three parameters, which are presented in Fig. 7. In addition, we have plotted in Fig. 7 the attractors for particular values of these parameters.

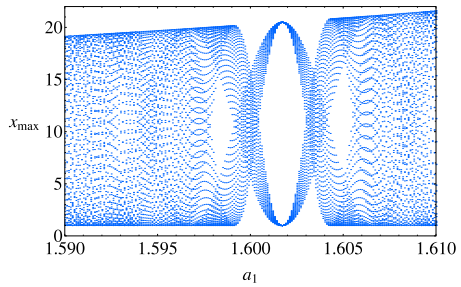

(a) $\mu = 1,\ a_2 = 0.25,\ m = \omega_0 = 1$

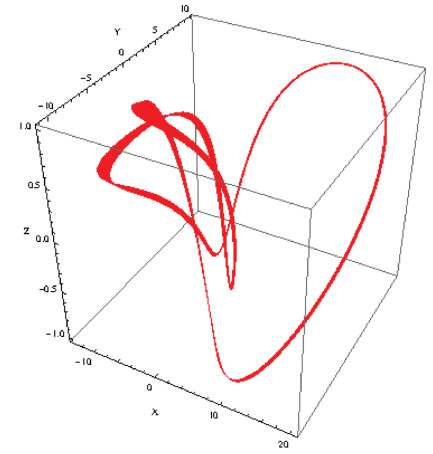

(b) $\mu = 1,\ a_1 = 1.6015,\ a_2 = 0.25,\ m = \omega_0 = 1$

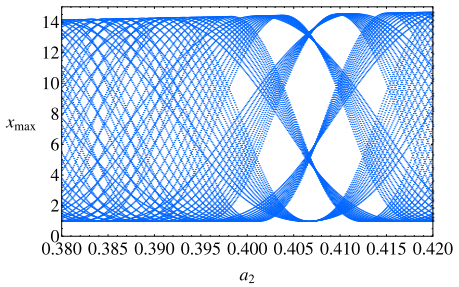

(c) $\mu = 1,\ a_1 = 1.5,\ m = \omega_0 = 1$

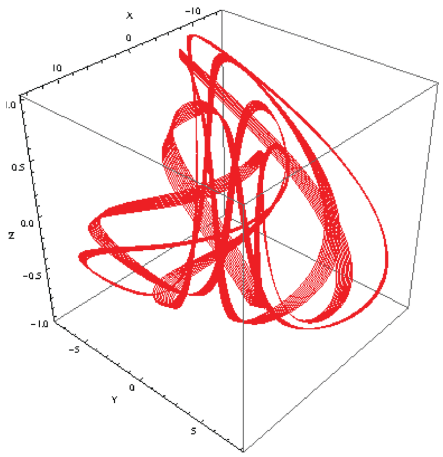

(d) $\mu = 1,\ a_1 = 1.5,\ a_2 = 0.405,\ m = \omega_0 = 1$

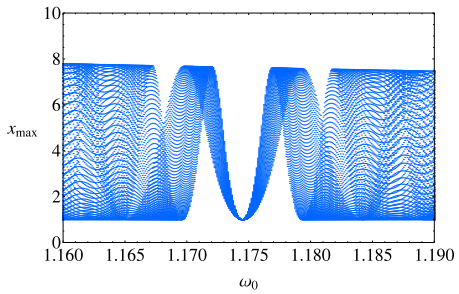

(e) $\mu = 1,\ a_1 = 1.5,\ a_2 = 0.25,\ m = 1$

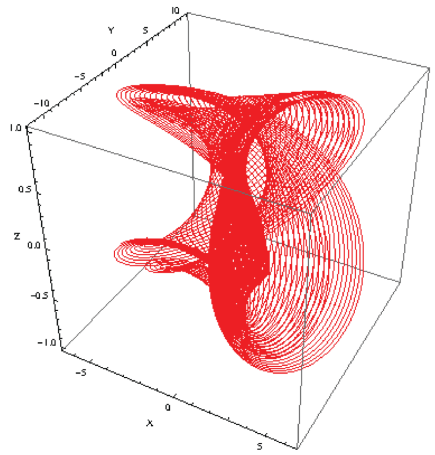

(f) $\mu = 1,\ a_1 = 1.5,\ a_2 = 0.25,\ \omega_0 = 1.618,\ m = 1$

FIG. 7. Bifurcation diagrams and phase portraits of model (4) for various values parameters. (a) $\mu = 1$, $a_2 = 0.25$, $m = \omega_0 = 1$. (b) $\mu = 1$, $a_1 = 1.6015$, $a_2 = 0.25$, $m = \omega_0 = 1$. (c) $\mu = 1$, $a_1 = 1.5$, $m = \omega_0 = 1$. (d) $\mu = 1$, $a_1 = 1.5$, $a_2 = 0.405$, $m = \omega_0 = 1$. (e) $\mu = 1$, $a_1 = 1.5$, $a_2 = 0.25$, $m = 1$. (f) $\mu = 1$, $a_1 = 1.5$, $a_2 = 0.25$, $\omega_0 = 1.618$, $m = 1$.

REFERENCES

[1]J.-P. Eckmann and D. Ruelle, "Ergodic theory of chaos and strange attractors," Rev. Mod. Phys. **57**, 617–656 (1985).
[2]V. S. Afraimovich and L. P. Shilnikov, "On invariant two-dimensional tori, their breakdown and stochasticity," in *Methods of the Qualitative Theory of Differential Equations* (Gorky State University, 1983), pp. 3–26. Translated in *American Mathematical Society Translations*, (2), Vol. 149 (1991), pp. 201–212.
[3]B. Muthuswamy and L. O. Chua, "Simplest chaotic circuit," Int. J. Bifurc. Chaos **20**(5), 1567–1580 (2010).
[4]J. Llibre and C. Valls, "On the integrability of a Muthuswamy-Chua system," J. Nonlinear Math. Phys. **19**(4), 477–488 (2012).
[5]J.-M. Ginoux, D. Lebiedz, R. Meucci, J. Llibre, and J. C. Sprott, "Flow curvature manifold and energy of generalized Liénard systems," Chaos, Solitons Fractals **161**, 112354 (2022).
[6]J.-M. Ginoux, R. Meucci, J. Llibre, and J. C. Sprott, "Energy function of 2D and 3D dynamical systems," Chaos, Solitons Fractals **190**, 115768 (2025).
[7]J.-M. Ginoux, R. Meucci, J. Llibre, and J. C. Sprott, "Energy function of 2D and 3D coarse systems," Chaos, Solitons Fractals **199**, 116643 (2025).
[8]C. N. Wang, Y. Wang, and J. Ma, "Calculation of Hamilton energy function of dynamical system by using Helmholtz theorem," Acta Phys. Sin. **65**(24), 240501 (2016).
[9]J. Ma, F. Wu, W. Jin, P. Zhou, and T. Hayat, "Calculation of Hamilton energy and control of dynamical systems with different types of attractors," Chaos **27**, 053108 (2017).
[10]J.-M. Ginoux, R. Concas, E. Pugliese, R. Meucci, and L. O. Chua, "From relaxation to chaotic oscillations: A new paradigm for memristor circuits," IEEE Trans. Circuits Syst. I Regul. Pap. **72**, 7160–7169 (2025).
[11]E. A. Coddington and N. Levinson, *Theory of Ordinary Differential Equations* (McGraw-Hill, New York, 1955).
[12]D. H. Kobe, "Helmholtz's theorem revisited," Am. J. Phys. **54**(6), 552–554 (1986).
[13]C. Sarasola, F. J. Torrealdea, A. d'Anjou, A. Moujahid, and M. Grana, "Energy balance in feedback synchronization of chaotic systems," Phys. Rev. E **69**, 011606 (2004).
[14]J. Yu, Z. T. Njitacke, D. Jiang, J. Wu, and J. Awrejcewicz, "Energy function and complex dynamics from a jerk system," Phys. Scr. **99**, 015245 (2024).
[15]M. Sandri, "Numerical calculation of Lyapunov exponents," Math. J. **6**, 78–84 (1996).
[16]G. Benettin, L. Galgani, A. Giorgilli, and J.-M. Strelcyn, "Lyapunov characteristic exponents for smooth dynamical systems and for Hamiltonian systems: A method for computing all of them. Part 2: Numerical application," Meccanica **15**, 21–30 (1980).
[17]M. Klein and G. Baier, "Hierachies of dynamical systems," in *A Chaotic Hierarchy*, edited by G. Baier and M. Klein (World Scientific, Singapore, 1991), pp. 1–25; see Table, p. 7.
[18]A. Wolf, J. B. Swift, H. L. Swinney, and J. A. Vastano, "Determining Lyapunov exponents from a time series," Physica D **16**, 285–317 (1985).
[19]S. Newhouse, D. Ruelle, and F. Takens, "Occurrence of strange Axiom A attractors near quasiperiodic flows on T^m, $m \geqslant 3$," Commun. Math. Phys. **64**(1), 35–40 (1978).
[20]N. Fenichel, "Persistence and smoothness of invariant manifolds for flows," Indiana Univ. Math. J. **21**, 193–226 (1971).
[21]M. S. Baptista and I. L. Caldas, "Dynamics of the two-frequency torus breakdown in the driven double scroll circuit," Phys. Rev. E **58**, 4413–4420 (1998).
[22]V. Arnold, V. Afraimovich, Y. Ilyashenko, and L. Shilnikov, "Bifurcation theory," in *Dynamical Systems V. Encyclopaedia of Mathematical Sciences*, edited by V. Arnold (Springer-Verlag, New York, 1994) (in Russian).
[23]R. O. Medrano-T, M. S. Baptista, and I. L. Caldas, "Shilnikov homoclinic orbit bifurcations in the Chua's circuit," Chaos **16**(4), 043119 (2006).
[24]E. Freire, A. J. Rodriguez-Luis, E. Gamero, and E. Ponce, "A case study for homoclinic chaos in an autonomous electronic circuit: A trip from Takens-Bogdanov to Hopf-Shilnikov," Physica D **62**(1–4), 230–253 (1993).
[25]A. Andronov and E. Leontovich, "Some cases of the dependence of the limit cycles upon parameters," Uchen. Zap. Gork. Gos. Univ. **6**, 3–24 (1939).
[26]A. Andronov, E. Leontovich, I. Gordon, and A. Maier, *Theory of Bifurcations of Dynamical Systems on a Plane* (Israel Program for Scientific Translations, Jerusalem, 1971).
[27]Y. A. Kuznetsov, *Elements of Applied Bifurcation Theory* (Springer-Verlag, New York, 1995), p. 632.
[28]R. Concas, A. Montori, E. Pugliese, A. Perinelli, L. Ricci, and R. Meucci, "Analysis of an improved circuit for laser chaos and its synchronization," IEEE Access **12**, 100602–100610 (2024).
[29]P. Caldirola, "Forze non conservative nella meccanica quantistica," Nuovo Cim **18**, 393–400 (1941).
[30]E. Kanai, "On the quantization of the dissipative systems," Prog. Theor. Phys. **3**(4), 440–442 (1948).
[31]P. Hamill, *A Student's Guide to Lagrangians and Hamiltonians* (Cambridge University Press, 2014).